Data-driven fuzzy logic approach for input admittance estimation in grid-tied inverters

Kamran Sabahi
Department of electronic systems
Aalborg University
Aalborg, Denmark 9220
ksabahi@es.aau.dk

Jesper Rindom Jensen
Department of electronic systems
Aalborg University
Aalborg, Denmark 9220
jrj@es.aau.dk

Yang Wu
Department of energy systems
Aalborg University,
Aalborg, Denmark 9220
yawu@energy.aau.dk

Xiongfei Wang
Department of energy systems
Aalborg University,
Aalborg, Denmark 9220
xiongfei@kth.se

Mads Græsbøll Christensen
Department of electronic systems
Aalborg University,
Aalborg, Denmark 9220
mgc@es.aau.dk

***Abstract*—Information about the input admittance of a three-phase grid connected inverter is important in stability assessment when connected to a power grid. However, existing neural network (NN)-based estimation methods typically require extensive training data and depend on frequency sweep as an additional input to generalize the estimation. This paper proposes a data-driven fuzzy logic system (FLS) for input admittance estimation of a three-phase grid-connected inverter, achieving generalization using only the system's operating points (OPs) as inputs, without requiring frequency information. By defining a limited set of rule bases, the transfer function (TF) coefficients of the input admittance are deduced as the FLS output, without requirement on extensive training data. Simulation results have confirmed the efficiency of the proposed method.**

Keywords— Input admittance, grid connected inverter, stability, fuzzy logic system and machine learning)

I. INTRODUCTION

In modern power systems, inverter-based resources (IBRs) are replacing traditional synchronous generators, playing a vital role in stability and reliability [1, 2]. Small-signal stability analysis, especially the admittance-based approach, is essential for identifying instabilities and measuring stability margins. This approach requires two main elements: the grid impedance and the IBR's input admittance [3]. While grid impedance can often be determined, estimating IBR admittance is more complex due to control loops operating at various time scales and limited vendor-provided details, especially in commercial IBRs like solar PV and wind farms [4, 5]. Admittance models also depend on operating conditions, which poses challenges [6]. To address this, both analytical and data-driven methods are used to create generalized admittance models [7]. Analytical methods are often impractical due to limited control information from vendors and complex calculations, making it difficult to address operating point (OP) dependency. Data-driven machine learning (ML) models, on the other hand, derive inverter admittance models based on training data, incorporating OPs and frequency sweep as inputs [8]. For example, recurrent neural network (RNN) [9] and feedforward neural network (NN) [10] have been applied to estimate system impedance, while support vector machine (SVM) approach [11] has been used in the DQ frame. Some methods use transfer learning or a two-stage approach combining offline modeling with online training to optimize performance [12, 13]. A stacked autoencoder-based framework was proposed for predicting impedance profiles of voltage source converters across various OPs, offering scalability for multi-converter systems and the ability to predict impedance at unstable points based solely on stable operation data [14]. Another approach uses a double deep neural network (DNN) to model impedance and estimate stability regions for grid-converter interaction systems [15]. That method addressed the challenge of varying OPs caused by fluctuating renewable energy, enabling accurate and fast online stability evaluation. Although these ML approaches effectively estimate input admittance based on operating points, their reliance on extensive training data and the need to incorporate a frequency sweep as an additional input to generalize the estimation add complexity, making them less practical for real-world applications.

Fuzzy logic systems (FLSs), as one of the significant tools in data-driven modeling methods, offer advantages over NNs when modeling a system with limited data [16]. By incorporating expert knowledge, they compensate for data scarcity, providing transparent models that handle uncertainty well. Their rule-based approach is conducive to small datasets, reducing the risk of over-fitting often seen in NNs [16]. This paper proposes an FLS to estimate the admittance of a grid-tied inverter, using OPs as inputs and deducing the numerator and denominator coefficients of the input admittance transfer function (TF) as outputs. The FLS is tuned using data obtained from grid-connected inverter simulations at selected OPs. At each OP, frequency scanning generates admittance Bode diagrams, from which numerator and denominator coefficients are extracted to directly define the consequent parameters and fuzzy rules. Unlike conventional ML methods, the proposed FLS: (1) builds rules with minimal data (no intensive training), and (2) generalizes across frequencies without sweep inputs.

The remainder of this paper is organized as follows: Section 2 discusses the input admittance calculation of a grid-connected inverter. The proposed FLS approach is introduced in Section 3, followed by simulation results in Section 4 and

conclusions in Section 5.

II. GRID CONNECTED INVERTERS AND THEIR INPUT ADMITTANCE

A typical configuration of a grid-connected inverter is illustrated in Fig 1. In this figure, considering a DC source, switching devices, the designed controllers and filters, if the input admittance has a nonnegative conductance at all frequencies, the inverter will hardly encounter instabilities. However, in practical applications, vendors of IBRs provide limited information regarding the hardware configurations and control algorithms of these IBRs. One approach to measuring the inverter's input admittance, treating it as a black box, is frequency response estimation. Known as the frequency scanning method, this technique injects sinusoidal signals in the DQ frame and analyzes the system's steady-state response.

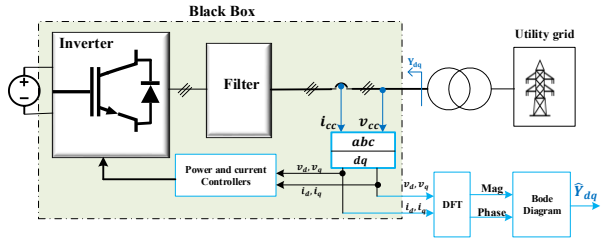

Fig 1: Schematic of a grid-tied inverter and the frequency scanning technique for input admittance estimation

The discrete Fourier transform (DFT) can be utilized to extract the amplitude and phase, ultimately obtaining the frequency response similar to a Bode diagram [17, 18]. The obtained Bode diagram can be represented in the DQ frame as follows:

$$Y_{dq} = \begin{bmatrix} y_{dd}(s) & y_{dq}(s) \\ y_{qd}(s) & y_{qq}(s) \end{bmatrix}, \quad (1)$$

where y_{dq} and y_{qd} represent the admittance's off-diagonal elements, while y_{dd} and y_{qq} denote the diagonal admittances in the d and q axes, respectively. Any element in the admittance model Eq. (1) can be expressed in the following general form, consisting of numerator and denominator polynomials [2, 10]:

$$Y_{dq}(s) = \begin{bmatrix} \frac{a_{dd,m_{11}}s^{m_{11}}+\cdots+a_{dd,1}s^1+a_{dd,0}}{s^{n_{11}}+\cdots+b_{dd,1}s^1+b_{dd,0}} & \frac{a_{dq,m_{12}}s^{m_{12}}+\cdots+a_{dq,1}s^1+a_{dq,0}}{s^{n_{12}}+\cdots+b_{dq,1}s^1+b_{dq,0}} \\ \frac{a_{qd,m_{21}}s^{m_{21}}+\cdots+a_{qd,1}s^1+a_{qd,0}}{s^{n_{21}}+\cdots+b_{qd,1}s^1+b_{qd,0}} & \frac{a_{qq,m_{22}}s^{m_{22}}+\cdots+a_{qq,1}s^1+a_{qq,0}}{s^{n_{22}}+\cdots+b_{qq,1}s^1+b_{qq,0}} \end{bmatrix}, \quad (2)$$

where m_{ij} and n_{ij} (for $i,j = 1,2$) represent the orders the of numerator and denominator of each TF, respectively, and $a_{\alpha\beta,m_{ij}}$ and $b_{\alpha\beta,n_{ij}}$ (for $\alpha, \beta \in (d,q)$) denote the matrix coefficients of the numerator and denominator.

When the grid impedance $Z_g(s)$ is known, stability can be evaluated by analyzing the poles of the characteristic polynomial of the inverter-grid system, given by

$$P_{IG} = \left[I + Y_{dq}(s)Z_g(s)\right]^{-1}. \quad (3)$$

However, the numerator and denominator coefficients of Y_{dq} vary with changes in the system's OPs, necessitating new measurements to update the matrix entries as conditions change. To illustrate this, the Bode diagram of $y_{qq}(s)$ is plotted in Fig 2 for three different OPs- OP#1, OP#2, and OP#3- for the IBR system shown in Fig 1. Note that these Bode diagrams can be obtained for the other admittance entries (y_{dd}, y_{dq}, and y_{qd}). The figure highlights that variations in OPs significantly affect both the magnitude and phase of $Y_{dq}(s)$. These variations can critically impact IBR stability (Eq.(3)). For each Bode diagram corresponding to the three OPs (OP#1, OP#2, and OP#3) depicted in Fig 2, the frequency response data (FRD) function was employed to fit TFs as represented in Eq. (2).

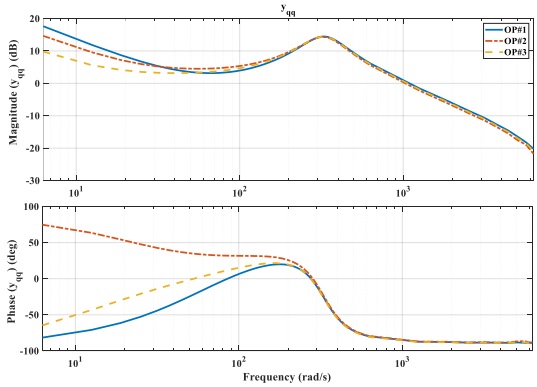

Fig 2: Bode diagram of y_{qq} for three different Ops

For OP#1, the fitted TF obtained with the FRD function is $y_{qq}(s) = \frac{s^2+15s+500}{s^3+200s^2+108s}$ with 95% accuracy. For OP#2, the fitted TF is $y_{qq}(s) = \frac{0.9s^2+13.5s-360}{s^3+160s^2+105s}$ with 99% accuracy, and for OP#3 is $y_{qq}(s) = \frac{16s^2+0.09s}{s^2+0.2s+110}$ with 97% accuracy. These results indicate that changes in the OP lead to variations in the numerator and denominator coefficients ($a_{\alpha\beta,m_{ij}}$ and $b_{\alpha\beta,n_{ij}}$), affecting the poles and zeros of the admittance matrix Y_{dq}. Since the numerator and denominator coefficients of Y_{dq} change with the operating point, continuously updating them is crucial for an accurate analysis of inverter-grid interactions. However, relying on new frequency-domain measurements each time is impractical, as the frequency-scanning method is both costly and time-consuming. To tackle this issue, feedforward neural network (NN)-based approaches were proposed in [19] to estimate input admittance across a wide range of operating conditions. The NN was trained on datasets representing admittance characteristics under various scenarios, and once trained, it can estimate both the real and imaginary components of the input admittance. However, their effectiveness depends on having a large and diverse training dataset, as well as incorporating an additional input, such as a 'frequency sweep,' to generalize the admittance calculations across different frequencies. This, in turn, adds complexity to their implementation.

To address these challenges, the following section proposes a data-driven method based on fuzzy logic systems (FLS) to overcome these limitations. This approach estimates the inverter's admittance using a much smaller training dataset and eliminates the need for a frequency sweep, thereby enhancing both efficiency and practicality. In the proposed FLS method, the OP serves as the input, while the outputs are the numerator and denominator coefficients of

Y_{dq} , enabling dynamic adaptation to varying operating conditions. It is also important to highlight that analyzing the poles and zeros of the transfer function, which can be accomplished using the proposed FLS method, offers valuable insights into inverter stability. For example, OP#2's TF has a zero in the right half-plane (RHP), which, when connected to a weak grid, could shift the root locus rightward, reducing stability and causes oscillations in the voltage and current at the point of common coupling (PCC) as illustrated (for phase a) in Fig 3.

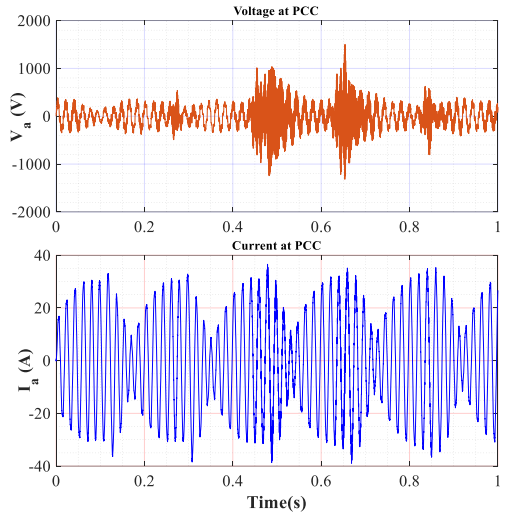

Fig 3. Voltage at PCC when the inverter with OP#2 connected to a weak grid

III. Proposed FLS for Admittance Estimation

FLSs provide a powerful approach for modeling complex systems and accurately estimating their outputs. They effectively handle the inherent uncertainty and imprecision present in real-world scenarios. By leveraging linguistic variables and fuzzy sets, FLSs can capture the complexities of system behavior, resulting in more precise modeling. Additionally, the adaptive nature of FLSs allows them to dynamically adjust to changing input conditions, ensuring reliable output estimations across diverse environments [16]. This flexibility makes fuzzy logic particularly effective for systems with incomplete or noisy data. In this context, since the coefficients of the admittance TF depend on the OPs of the IBR, the goal is to utilize an FLS to estimate these coefficients over a wide frequency range. The overall structure of the proposed FLS-based admittance estimation method is shown in Fig 4.

In this framework, the designed FLS takes the OPs as input and applies fuzzification, fuzzy inference, and defuzzification based on predefined rules to determine the input admittance coefficients $a_{\alpha\beta,m_{ij}}$ and $b_{\alpha\beta,n_{ij}}$. The estimated $Y_{dq}(s)$ is then obtained and used to assess the stability of the inverter-grid connection. In the proposed method, a Mamdani-type FLS is employed to formulate the IF-THEN rules for estimating the numerator and denominator coefficients of $y_{qq}(s)$ in the grid-tied inverter are formulated as follows:

If P is P_1 and Q is Q_1 THEN $a_{qq,i}$ is a^*_{qq} and $b_{qq,j}$ is b^*_{qq}, (4)

where P_1 and Q_1 are linguistic variables (antecedent part) and a^*_{qq} and b^*_{qq} (in the vector form) denote the numerator and denominator coefficients (consequent part) of the corresponding admittance TF.

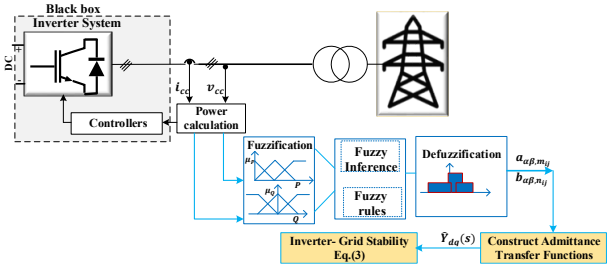

Fig 4: The proposed FLS-based admittance estimation of IBRs

The FLS tuning process comprises two main stages: (1) designing the antecedent MFs based on expert knowledge, and (2) determining the consequent crisp MFs and rule base through systematic simulations of the grid-connected inverter (nine simulations).

Given the known operational range of the antecedent parts (active and reactive powers), three MFs—labeled as small (P_S, Q_S), medium (P_M, Q_M), and large (P_L, Q_L) (see Fig 5) — are defined for each input. In this study, the Medium MFs are centered at nominal values of $P_o = 5Kw$ and $Q_0 = 0Kvar$. The Small and Large MFs are symmetrically offset by Δ_0= $5Kw$ and Δ_1= $4Kvar$, respectively, to effectively capture the full range of input variations. This uniform partitioning of the input space facilitates effective fuzzy rule formulation. The FLS utilizes three MFs per input, resulting in nine rules (as specified in Eq.(4)).

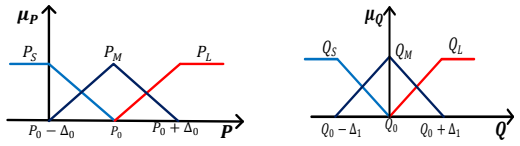

Fig 5: Input MFs for the proposed FLS

To determine the consequent MFs (modeled as crisp numbers), nine simulations were performed under distinct operating conditions: at the nominal points (P_o, Q_o) and their variations ($P_o \pm \Delta_0$, $Q_o \pm \Delta_1$).

Table 1: derived rule bases for the proposed FLS-based admittance estimation method

	P_S	P_M	P_L
Q_S	$a_{dd,2}=0.2, a_{dd,1}=108, a_{dd,0}=0$ $b_{dd,2}=1, b_{dd,1}=14, b_{dd,0}=428$	$a_{dd,2}=1, a_{dd,1}=0.2, a_{dd,0}=108$ $b_{dd,2}=0, b_{dd,1}=0.1, b_{dd,0}=13.6$	$a_{dd,3}=1, a_{dd,2}=200, a_{dd,1}=108, a_{dd,0}=0,$ $b_{dd,2}=0.9, b_{dd,1}=12.5, b_{dd,0}=-460$
Q_M	$a_{dd,3}=1, a_{dd,2}=200, a_{dd,1}=108, a_{dd,0}=0$ $b_{dd,2}=1, b_{dd,1}=15, b_{dd,0}=500$	$a_{dd,2}=1, a_{dd,1}=0.2, a_{dd,0}=109$ $b_{dd,2}=0, b_{dd,1}=0.1, b_{dd,0}=14$	$a_{dd,3}=1, a_{dd,2}=160, a_{dd,1}=105, a_{dd,0}=0$ $b_{dd,2}=0.9, b_{dd,1}=13.5, b_{dd,0}=-360$
Q_L	$a_{dd,2}=108, a_{dd,1}=200, a_{dd,0}=0$ $b_{dd,2}=1, b_{dd,1}=16, b_{dd,0}=600$	$a_{dd,2}=1, a_{dd,1}=0.2, a_{dd,0}=110$ $b_{dd,2}=16, b_{dd,1}=0.04, b_{dd,0}=0$	$a_{dd,2}=1, a_{dd,1}=0.2, a_{dd,0}=100$ $b_{dd,2}=14, b_{dd,1}=0.1, b_{dd,0}=0$

For each simulation scenario where the inverter operates at specific active and reactive power levels ((P_S, Q_S), (P_M, Q_M), and (P_L, Q_L)), a Bode diagram is generated. From each Bode plot, the TF's numerator and denominator coefficients are extracted. The consequent parameters derived from these simulations are summarized in Table 1, thereby establishing the complete rule base for the FLS model.

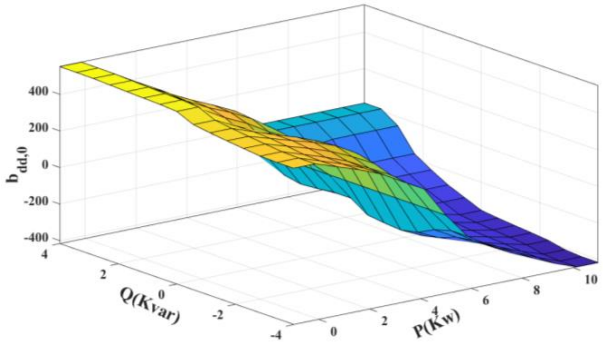

Fig 6: Control surface for the denominator coefficients $b_{dd,0}$

It should be noted that in this table, fuzzy rules related to y_{qq} of the admittance matrix are provided due to its importance. However, similar rules can be defined for other elements of the admittance matrix. The control surfaces for the denominator coefficients $b_{dd,0}$, which play a crucial role in the stability analysis of the system, are shown in Fig 6. By examining these surfaces, one can observe the relationship between the input variables and the resulting coefficients, providing valuable insights into the system's stability under varying operating conditions.

IV. Simulation Results

The goal of this section is to demonstrate that the proposed FLS-based admittance estimation can generalize to various OPs beyond those specifically used to define the rules. In addition to the proposed FLS-based admittance estimation, a comparison has been made with results obtained from the feedforward NN [8]. Unlike the FLS method, where the rule bases are designed using specific OPs, the feedforward NN incorporates not only the OPs of the system but also the frequency sweep as an additional input to generalize the model. The output of feedforward NN is designed to estimate both the real and imaginary components of the admittance at the specified frequency. This feedforward NN was trained, validated, and tested using a comprehensive dataset with sufficient data points to ensure robust performance.

Case 1: For OP with $P_1 = 9Kw$ and $Q_1 = -2.5Kvar$, the performance of the proposed FLS method is compared to feedforward NN-based methods, with results presented in Fig 7 and Table 2. From these results, it is evident that the FLS method outperforms the NN-based approach, particularly at lower frequencies in the phase diagram. These low frequencies are crucial for sub-synchronous stability analysis, making the FLS method more effective in this context. Additionally, the FLS method offers improved accuracy while requiring fewer training data and eliminating the need for a frequency sweep to generalize admittance estimation, further enhancing its suitability for online applications. The FLS utilizes the firing strengths of four rules (2, 3, 5, and 6), with rules 3 and 6 having the highest influence. The derived coefficients are $a_{dd,2} = 165$, $a_{dd,1} = 109$, $a_{dd,0} = 54$, and $b_{dd,2} = 1$, $b_{dd,1} = 11.5$, and $b_{dd,0} = -325$, resulting in a zero in the RHP. These coefficients demonstrate the generability of the proposed FLS, as the corresponding OP results in a zero in the RHP, consistent with the rules defined in Table 1. Given these coefficients, careful consideration is required when connecting this inverter—operating under the mentioned OPs—to a weak grid, as it may cause oscillations in the current and voltage at the PCC.

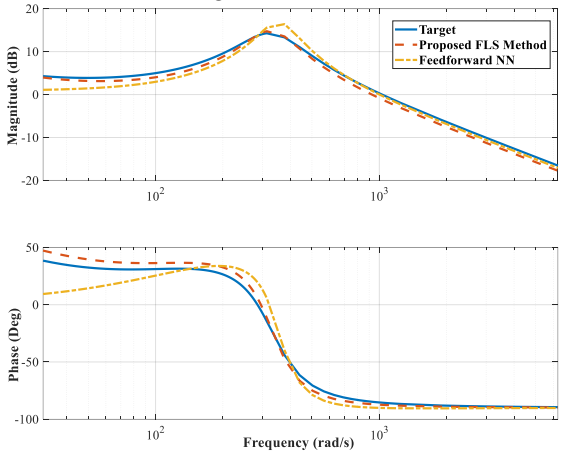

Fig 7: the estimated $y_{qq}(s)$ using the proposed FLS and feedforward NN methods for the first case

Specifically, when the inverter is connected to a grid with an impedance of $Z_g = 1 + 5 \times 10^{-3}s$, instability in the PCC voltage and current occurs, with the current in the DQ frame depicted in Fig 8. This figure clearly illustrates how weak grid conditions can trigger oscillations in the inverter-grid connection, emphasizing the need for thorough stability evaluations in such scenarios.

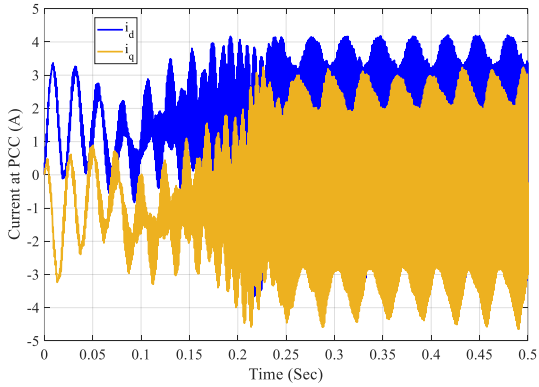

Fig 8. Currents at PCC for the inverter-grid system in case 1

Case 2: For OP $P_2 = 2.5Kw$ and $Q_2 = -1Kvar$, the estimated admittance results obtained using the proposed FLS method and the NN-based method are presented in Fig 9 and Table 2. The results clearly demonstrate the efficiency of the proposed method. For this OP, the activated FLS rules (1, 2, 4, and 5) yield the following coefficients: $a_{dd,2} = 200$, $a_{dd,1} = 1069$, $a_{dd,0} = 109$, and $b_{dd,2} = 1$, $b_{dd,1} = 19.5$, and $b_{dd,0} = 110$. Unlike case 1, the inverter admittance here does not have a zero in the RHP which is consistent with the defined rules in Table 1. This demonstrates the FLS method's ability to ensure stable operation across different OPs, while also highlighting its key advantages: it neither requires large amounts of training data nor a frequency sweep as an additional input, as needed by the NN-based method. Furthermore, a simulation is conducted to verify the stability of the inverter (with the OPs in Case 2) when connected to

the grid with the impedance given in Case 1.

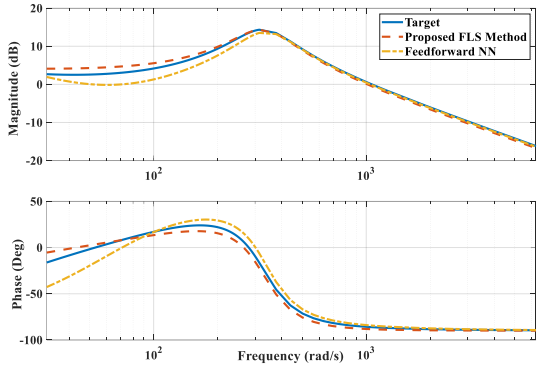

Fig 9: the estimated $y_{qq}(s)$ using the proposed FLS and feedforward NN methods for the second case

Table 2: MAPE index comparison of FLS and feedforward NN methods

	Proposed FLS method		Feedforward NN method	
	Magnitude	**Phase**	**Magnitude**	**Phase**
Case 1	5.13%	6.08%	7.78%	17.58%
Case 2	2.21%	3.18%	6.45%	17.51%

Unlike in Case 1, where instability occurred due to a RHP zero in the admittance TF, the coefficients in this case remain positive, ensuring a stable connection. The simulation results, presented in Fig 10, confirm that the PCC current remains stable, further demonstrating the effectiveness of the proposed FLS method in maintaining stability across different operating conditions.

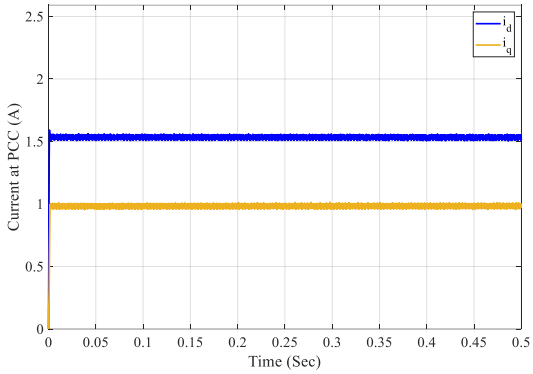

Fig 10. Currents at PCC for the inverter-grid system in case 2

V. Conclusion

In this paper, a novel data-driven FLS-based approach has been developed for estimating the input admittance of a three-phase grid-connected inverter. In the proposed method, the OPs of the system are used as inputs to the FLS, which then deduces the numerator and denominator coefficients of the inverter's input admittance transfer function. The rule bases of the proposed FLS are defined using limited measurements carried out in the DQ frame. Compared to existing feedforward NN-based methods, the proposed strategy requires limited training data and eliminates the need for additional inputs such as frequency sweeps, enhancing its suitability for online applications. Future studies will focus on experimental FLS training and real-time deployment for grid-tied inverters.

VI. References

[1] L. Xiong, X. Liu, Y. Liu, and F. Zhuo, "Modeling and stability issues of voltage-source converter-dominated power systems: A review," *CSEE Journal of Power and Energy Systems,* vol. 8, no. 6, pp. 1530-1549, 2020.

[2] L. Fan, Z. Miao, P. Koralewicz, S. Shah, and V. Gevorgian, "Identifying DQ-domain admittance models of a 2.3-MVA commercial grid-following inverter via frequency-domain and time-domain data," *IEEE Transactions on Energy Conversion,* vol. 36, no. 3, pp. 2463-2472, 2020.

[3] W. Zhou, M. H. Ravanji, N. Mohammed, and B. Bahrani, "Rapid Admittance Measurement of Power Converters Using Double-PLL Grid-following Inverters," *IEEE Transactions on Power Delivery,* 2024.

[4] L. Harnefors, M. Bongiorno, and S. Lundberg, "Input-admittance calculation and shaping for controlled voltage-source converters," *IEEE transactions on industrial electronics,* vol. 54, no. 6, pp. 3323-3334, 2007.

[5] Y. Zhu, J. Zhao, Z. Zeng, L. Mao, and K. Qu, "Impedance remodeling control strategy of grid-connected inverter with inertia-damping phase-locked loop under extremely weak grid," *International Journal of Electrical Power & Energy Systems,* vol. 158, p. 109961, 2024.

[6] W. Zhou, N. Mohammed, and B. Bahrani, "Operating-Point-Parameterized State-Space Models of Black-Boxed Grid-Following Inverters for Maximum Transferable Active Power Prediction," *IEEE Transactions on Industrial Electronics,* 2024.

[7] H. Wu, F. Zhao, and X. Wang, "A survey on impedance-based dynamics analysis method for inverter-based resources," *IEEE Power Electronics Magazine,* vol. 10, no. 3, pp. 43-51, 2023.

[8] M. Zhang, X. Wang, D. Yang, and M. G. Christensen, "Artificial neural network based identification of multi-operating-point impedance model," *IEEE Transactions on Power Electronics,* vol. 36, no. 2, pp. 1231-1235, 2020.

[9] P. Xiao, G. K. Venayagamoorthy, K. A. Corzine, and J. Huang, "Recurrent neural networks based impedance measurement technique for power electronic systems," *IEEE Transactions on Power Electronics,* vol. 25, no. 2, pp. 382-390, 2009.

[10] Y. Liao *et al.*, "Neural network design for impedance modeling of power electronic systems based on latent features," *IEEE Transactions on Neural Networks and Learning Systems,* 2023.

[11] N. Mohammed, W. Zhou, B. Bahrani, and D. J. Hill, "Support vector machines for predicting the impedance model of inverter-based resources," *IEEE Transactions on Power Systems,* 2024.

[12] Y. Li *et al.*, "Machine Learning At the Grid Edge: Data-Driven Impedance Models for Model-Free Inverters," *IEEE Transactions on Power Electronics,* 2024.

[13] M. Zhang, Y. Zhang, and Q. Xu, "Transfer learning based online impedance identification for module multilevel converters," *IEEE Transactions on Power Electronics,* 2023.

[14] Y. Wu *et al.*, "Impedance Profile Prediction for Grid-Connected VSCs with Data-Driven Feature Extraction," *IEEE Transactions on Power Electronics,* 2024.

[15] M. Zhang and Q. Xu, "Deep Neural Network-Based Stability Region Estimation for Grid-Converter Interaction Systems," *IEEE Transactions on Industrial Electronics,* 2024.

[16] J. M. Mendel, *Explainable Uncertain Rule-Based Fuzzy Systems*. Springer, 2024.

[17] H. Gong, X. Wang, and D. Yang, "DQ-frame impedance measurement of three-phase converters using time-domain MIMO parametric identification," *IEEE Transactions on Power Electronics,* vol. 36, no. 2, pp. 2131-2142, 2020.

[18] G. Francis *et al.*, "Algorithm and implementation system for measuring impedance in the dq domain," ed: Google Patents, 2015.

[19] M. Zhang, Q. Xu, and X. Wang, "Physics-informed neural network based online impedance identification of voltage source converters," *IEEE Transactions on Industrial Electronics,* vol. 70, no. 4, pp. 3717-3728, 2022.